

Reply to Reviewer #3

Understanding how aerosol particle age during transport is critically important for improving model performance yet still suffers from the paucity of field data that can guide model development. The current manuscript by Zhang et al., provides much needed property and aging data on PM_{2.5} particles by being able to compare the pathway impacts over inland vs the sea. To carry out this study, the authors examined the microphysical and optical properties of haze particles from the North China Plain (NCP) to the Yangtze River Delta (YRD) where cold fronts exhibited two different pathway: an inland path and a “sea” path that took the air mass across the East China Sea. The authors report that the “dryish” inland path favors a heterogeneous-centric aging pathway with single-core embedded soot, whereas the sea pathway, with its concomitantly very high RH and cloud processing favors entrainment and coalescence resulting in the production of super micron particles characterized by multiple soot cores inside large droplets/residuals that exhibit a lower absorption enhancement than that calculated for the inland pathway particles. This manuscript tackles an important problem with a modern, multi-method approach and yields novel, physically meaningful insights about how transport environment affects soot aging and absorption. This manuscript is recommended for publication AFTER some moderate revisions that are focused on clarifying the uncertainties and representativeness in the measurements, greatly increasing the language transparency in discussing the cloud process aging as the dominate mechanism vs. other high RH processes and increasing the narrative on the underlying modeling assumptions. These are discussed below. Also, the narrative is convoluted at several points within the manuscript and thus the authors are encouraged to have the manuscript grammar reviewed.

We are grateful for this reviewer’s comments. These comments are all valuable and helpful for improving our paper. We added a figure to indicate the representativeness of the transboundary transport event through the sea pathway (Figure S4). We added the standard deviation of the number fraction, D_p/D_c , and D_f in Figure 4, 7, 9. We also added the significant difference of D_p/D_c of soot-containing particles during two transport events and made the scales on

the ordinates same in Figure 7. We added a satellite image to indicate the presence of clouds along the sea transport pathway (Figure S7). We calculated the volume ratio of soot coatings to soot cores ($V_{coating}/V_c$) in Table S2. We added a sensitivity test to show the credibility of 72% $\Delta E_{abs}/\Delta(D_p/D_c)$ reduction (Figure S9). The manuscript grammar was also reviewed. Moreover, we answered the comments carefully and have made corrections in the submitted manuscript and supplementary information. The corrections and the responses are as following:

In the revised manuscript and supplementary information, the red color was marked as the revised places.

1. The analysis rests primarily on two winter haze events (2017, 2020). These events appear well chosen and documented, but they still represent a limited sample of meteorological regimes. How representative are these case studies and to what extent are they generalizable to other years, and source composition (e.g., wildfire aerosols vs fossil fuel)? It is assumed that the transport trajectories indicate that the haze plumes stayed in the boundary layer and did not punch through to the free troposphere.

Reply: We appreciated the reviewer's comments. Our previous studies investigated some transboundary transport haze events from the NCP to the YRD across inland areas (Zhang et al., 2023; Zhang et al., 2021). Their meteorological fields were similar to those of the transboundary transport event through the inland pathway in this study, that is strong northerly winds over eastern China under the influence of the Siberian cold high. In recent years, we have found that as the position of the high-pressure system shifts, haze aerosols from the NCP can be transported to the YRD through the sea pathway. Such transport patterns were observed not only in the second event but also during other time periods (Figure S4). Previously, only a limited number of modeling studies had identified this transport route (Wu et al., 2022). Moreover, we found that the chemical composition of the transported haze aerosols was similar in several transport events, with

secondary inorganic ions and organic matter being the dominant components. This is consistent with previous studies on other transboundary transport haze events from the NCP to the YRD (Huang et al., 2020; Li et al., 2019; Xie et al., 2023). Therefore, we can confirm that these two events are representative cases of transboundary transport of haze pollutants from the NCP to the YRD through the inland and the sea pathways. We added representative explanations.

P11 L275-277: “This meteorological field was similar to those of transboundary transport haze events from the NCP to the YRD across inland areas (Hou et al., 2020; Hu et al., 2021; Zhang et al., 2023).”

P11 L281-282: “Such wind patterns were observed not only in the second event but also in other periods, as shown in Figure S4.”

P12 L305-309: “This is consistent with previous studies on the transboundary transport of haze aerosols from the NCP to the YRD (Huang et al., 2020; Li et al., 2019; Xie et al., 2023). In summary, we can confirm that these two events represent typical cases of transboundary transport of haze pollutants from the NCP to the YRD through the inland and the sea pathways.”

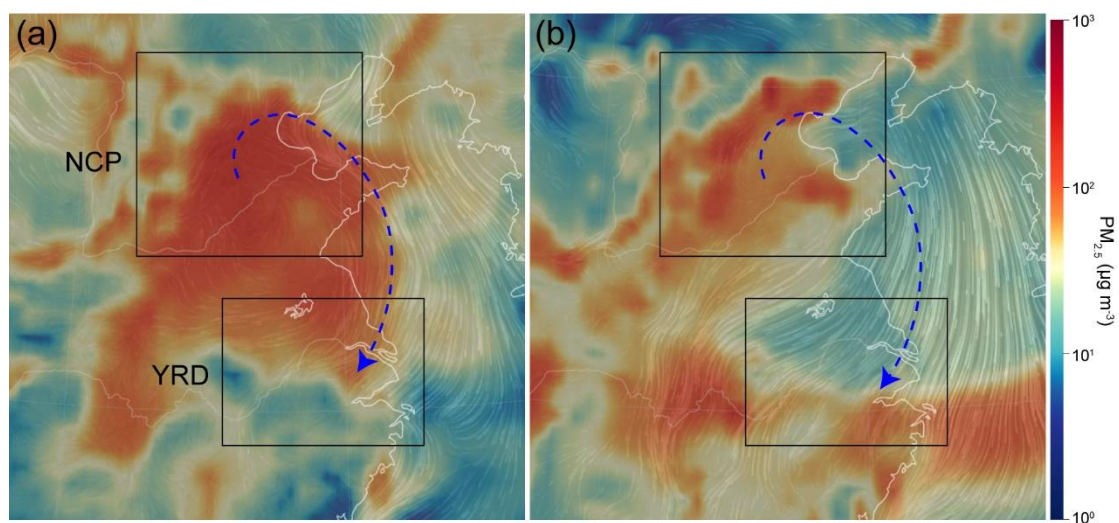


Figure S4. Wind fields combined with surface PM_{2.5} concentrations in eastern China. (a) 11:00 (local time) on January 4, 2020. (b) 4:00 (local time) on February 8, 2021.

2. While the Reviewer appreciates the effort of analyzing 3642 particles, the authors need to ascribe uncertainties/confidence intervals on all reported fractions (e.g., 62 vs. 67%; 71 vs. 72%) and on D_p/D_c and D_f . It is also suggested that a statistical significance test be performed in the comparison between inland and sea cases.

Reply: Thanks for the reviewer's comments. We added the standard deviation of the number fraction, D_p/D_c , and D_f in Figure 4, 7, 9 and the manuscript. We also added the significant difference of D_p/D_c of soot-containing particles during two transport events in Figure 7.

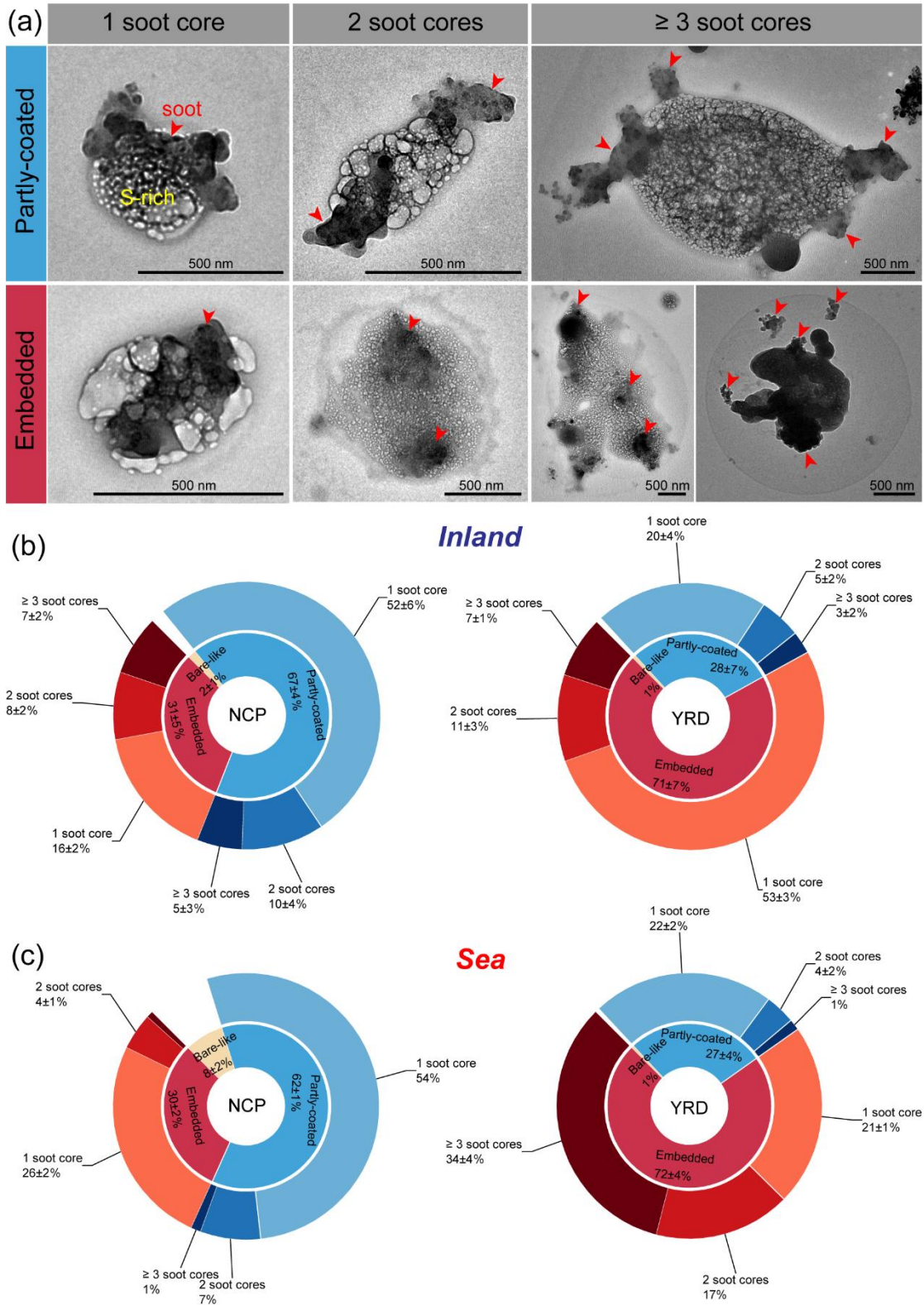


Figure 4. Typical TEM images and number fractions of soot-containing particles with different mixing structures and soot core numbers in two types of transboundary transport models from the NCP to the YRD. (a) Partly-coated and embedded soot-containing particles with different numbers of soot cores. (b)

Variation in the number fraction of soot-containing particles during the transboundary transport through the inland pathway. (c) Variation in the number fraction of soot-containing particles during the transboundary transport through the sea pathway.

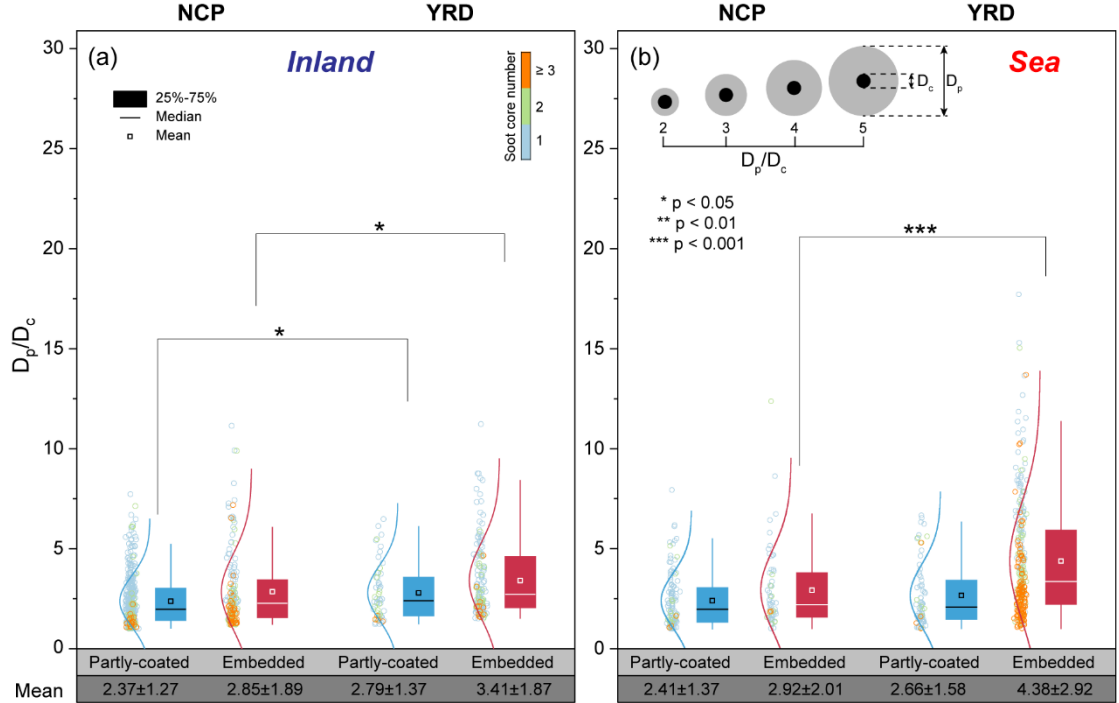


Figure 7. The size ratio of soot-containing particles to their soot cores (D_p/D_c) in two types of transboundary transport models from the NCP to the YRD. (a) D_p/D_c ratios of soot-containing particles transported through the inland pathway. (b) D_p/D_c ratios of soot-containing particles transported through the sea pathway. A schematic model of the D_p/D_c ratio of soot-containing particles with the core-shell structure is exampled.

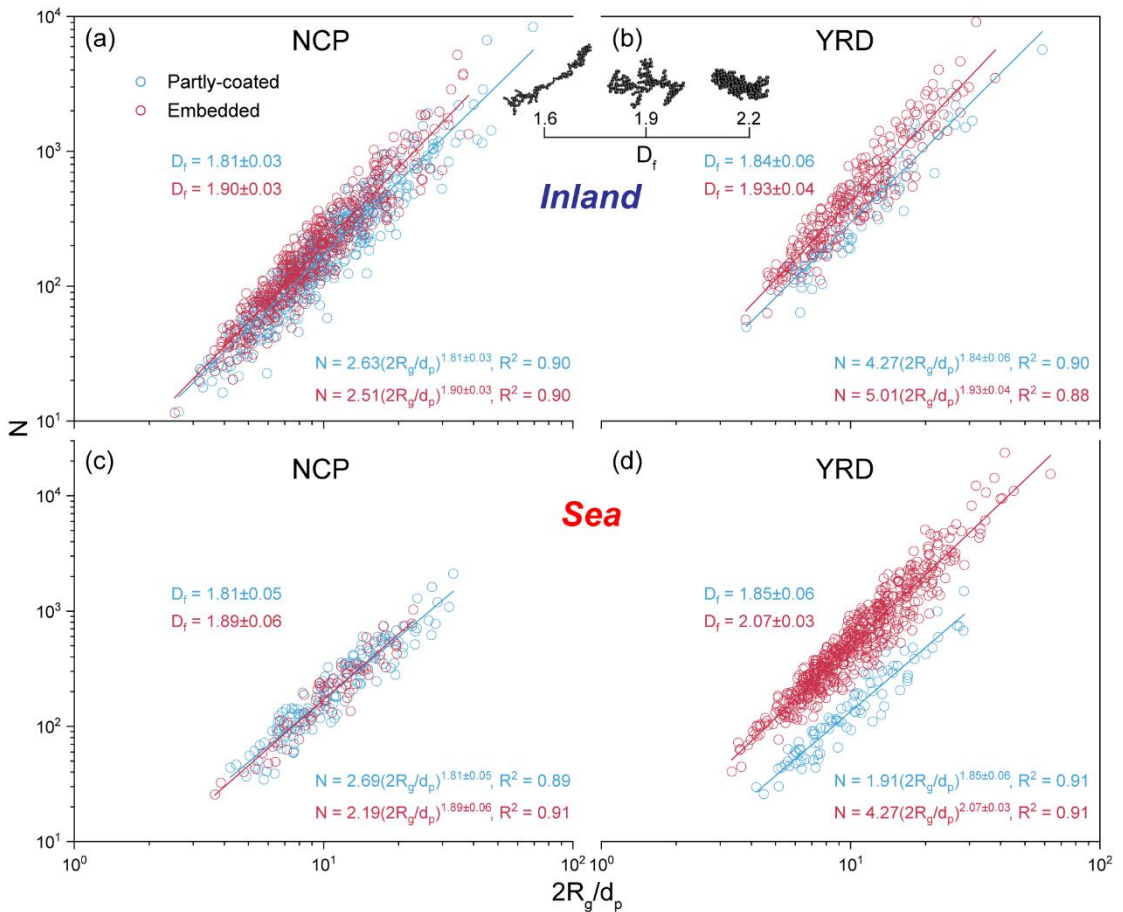


Figure 9. Variation in the fractal dimension (D_f) of partly-coated and embedded soot particles during their transboundary transport from the NCP to the YRD. (a-b) D_f of soot particles transported through the inland pathway. (c-d) D_f of soot particles transported through the sea pathway. A schematic model of the soot D_f is exemplified.

3. While the observation of water rims and droplet-like morphologies are compelling indicators of aqueous processing, they do not uniquely prove that cloud processing is indeed the route. One could observe similar water rims from deliquesced aerosol under very high RH below cloud. Indeed, the latter only requires a very high RH condition, similar to that reported, whereas the former requires supersaturation conditions for cloud droplet formation, which is not discussed in the manuscript. Thus, the authors need to clarify the distinction between in-cloud vs. sub-cloud aqueous processing as opposed to simply citing “cloud process”. Similarly, while it is reasonable to assume that multiple

cores (2 - 3) per particle are primarily due to cloud entrainment and collision-coalescence, other pathways (e.g., coagulation in a wet aerosol layer, co-injection and growth of BC-rich, organic-rich droplets) could contribute. Therefore, the authors are encouraged to provide a narrative (argument) that simple coagulation of soot-containing particles in a high-RH boundary layer is insufficient to produce the observed size and multicore distributions thereby supporting the proposed cloud droplet pathway. Similarly, the authors are encouraged to be more tempered with their statement (page 20; lines 550 - 551) that “cloud process aging under extremely high RH became them major evolution mechanisms.” An extremely high RH environment does not necessarily mean a cloud droplet environment (supersaturation conditions).

Reply: Thanks. As the reviewer commented, the water rim and droplet-like morphology are not direct evidence of soot-containing particles undergoing cloud processes. These phenomena can also be observed under non-supersaturated high RH conditions. Furthermore, we agree with the reviewer’s comment that other physicochemical pathways could also lead to multicore states in soot-containing particles, similar to cloud processes. Therefore, we have carefully considered the reviewer’s suggestion by adding a discussion on the variation of particle size distribution. We also emphasized that simple coagulation of soot-containing particles in high RH environments was insufficient to explain the observed particle sizes and multicore characteristics, supporting the role of cloud processing. Additionally, we added a satellite image to further indicate the presence of clouds along the transport pathway (Figure S7). The sentence in lines 550-551 has also been revised as suggested.

P18 L468-478: “It is noted that the peak diameter and core number of embedded soot-containing particles largely shifted from 446 nm and 1 to 925 nm and ≥ 3 during transboundary transport through the sea pathway (Figures 4c and 6c-d). The evolution implies that simple coagulation or condensation was not the primary aging processes of soot-containing

particles in high RH environments, because these mechanisms are insufficient to explain the observed micron-sized particles with multiple cores (Liu et al., 2018). Instead, cloud processing likely played a more important role. Figure S7 shows the satellite image combined with the backward trajectory of haze masses during December 7-8, 2020. We found the presence of clouds over the East China Sea during the transport of haze masses through the sea pathway (Figure S7).”

P23 L623-625: “When soot-containing particles were transported through the sea pathway, cloud process aging became their major evolution mechanisms.”

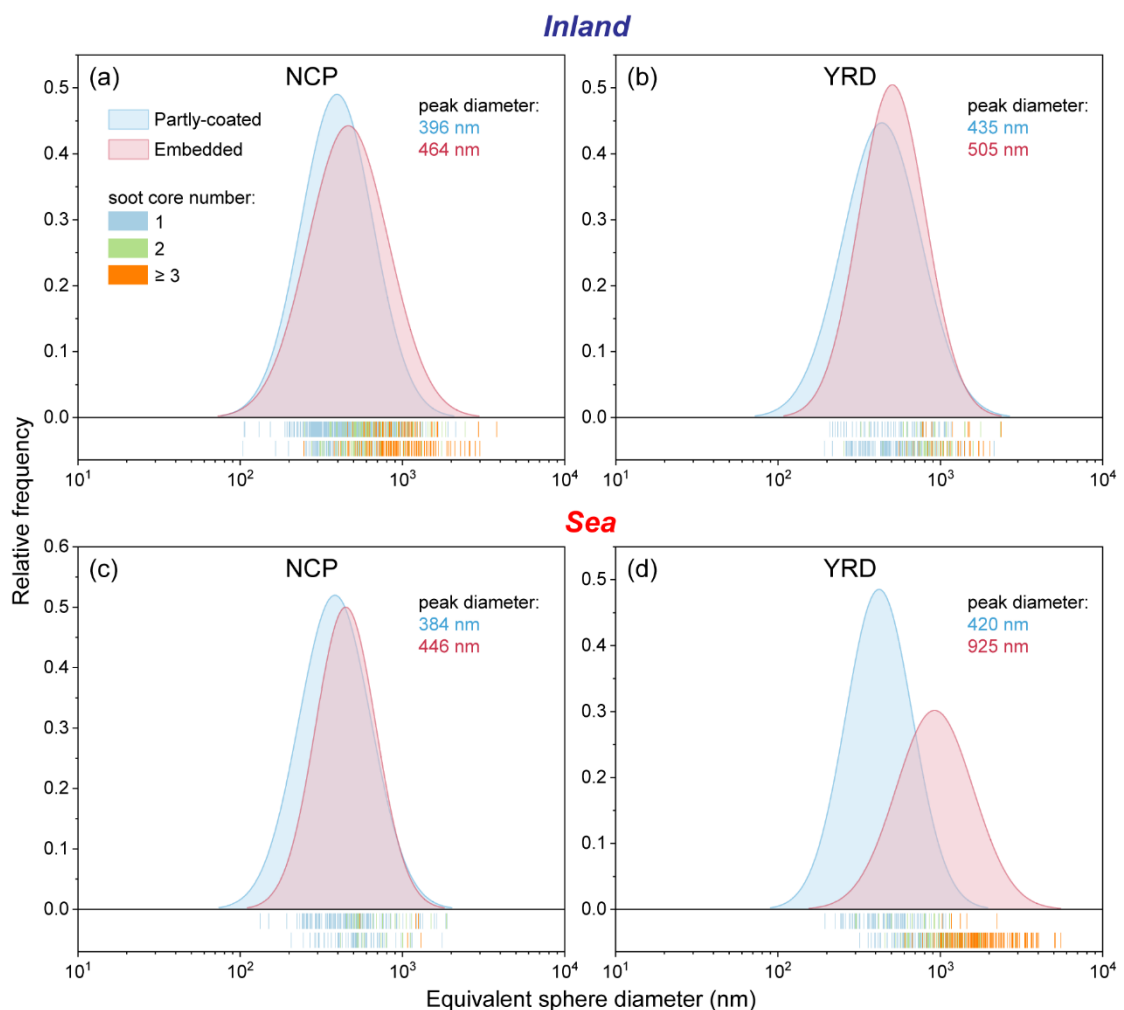


Figure 6. Number size distribution of soot-containing particles in two types of transboundary transport models from the NCP to the YRD. (a-b) Size distribution of soot-containing particles transported through the inland pathway. (c-d) Size

distribution of soot-containing particles transported through the sea pathway.

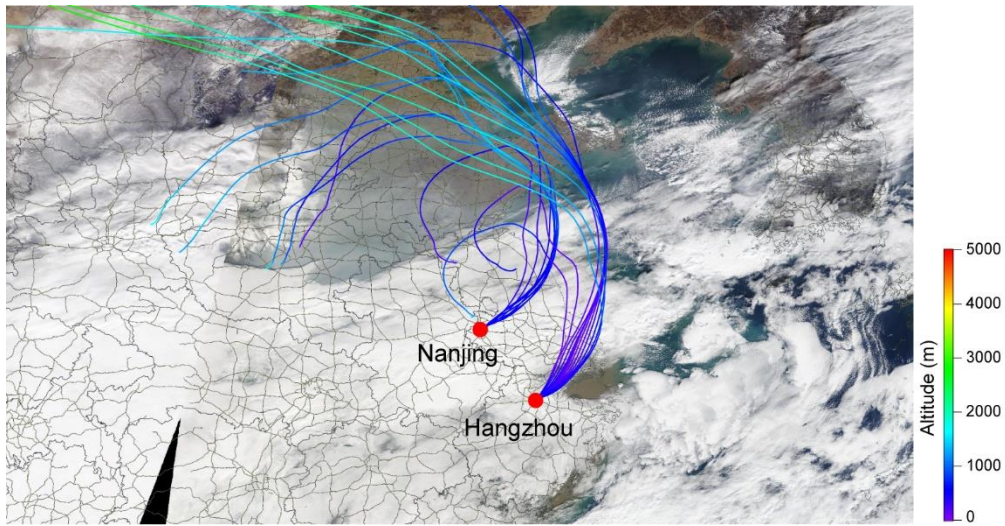


Figure S7. A satellite image combined with the backward trajectory of haze masses before arriving at Nanjing and Hangzhou sites during December 7-8, 2020.

4. While D_p/D_c is conventional for submicron size particles with a single-core BC, it is not the most robust choice for the super-micron, cloud-processed, multicore particles that dominate this study. In this size regime that is the focus of this study, D_p and D_c are both equivalent diameters derived from 2D projections of highly irregular, droplet-like particles and compacted aggregates. A major consequence of this is that D_p/D_c becomes strongly sensitive to particle morphology, orientation on the substrate, and, potentially, how the particle dried. Thus, the authors are encouraged to consider using the mass (or volume) ratio of coating to core, which is particle morphology agnostic. As a added benefit, the EMBS-DDSCAT framework used by the authors provides explicit core and matrix volumes for the modeled particles, thereby making it straightforward to examine optical enhancement versus coating:core mass (or volume) ratio instead of versus D_p/D_c . Finally, as cited above, error analysis is strongly suggested for this metric.

Reply: Thanks. In this study, to obtain the 3D diameter of particles, we established a correlation between the 2D diameter and the 3D diameter of particles using atomic force microscopy (AFM). This correlation enables the

estimation of the 3D diameter of soot-containing particles. The employment of the 3D diameter can reduce the influence of particle morphology and the substrate on the D_p/D_c ratio. To make the results more straightforward, we calculated the volume ratio of soot coatings to soot cores ($V_{coating}/V_c$) in Table S2. The error (i.e., standard deviation) of D_p/D_c was also provided in Figure 7.

P8 L200-201: “The volume ratio of soot coatings to soot cores ($V_{coating}/V_c$) was further calculated according to the D_p/D_c .”

P16 L417-419: “The D_p/D_c and $V_{coating}/V_c$ ratios of transboundary soot-containing particles were calculated to reflect the coating thickness of soot particles and to quantify the aging degree of soot particles (Figure 7 and Table S2).”

P16 L422: “Correspondingly, the mean $V_{coating}/V_c$ ratios remained at 12-13 and 22-24 (Table S2).”

P16 L426-427: “Their mean $V_{coating}/V_c$ ratios also increased from 12 and 22 in the NCP to 21 and 39 in the YRD (Table S2).”

P17 L449-451: “Consistently, the mean $V_{coating}/V_c$ ratios increased from 13 for the partly-coated structure and 24 for the embedded structure to 18 and 83 (Table S2).”

Table S2. The mean volume ratio of soot coatings to soot cores ($V_{coating}/V_c$) in two types of transboundary transport models from the NCP to the YRD.

Transport pathway	Region	Particle type	$V_{coating}/V_c$
Inland	NCP	Partly-coated	12
		Embedded	22
	YRD	Partly-coated	21
		Embedded	39
Sea	NCP	Partly-coated	13
		Embedded	24
	YRD	Partly-coated	18
		Embedded	83

5. There is the implicit assumption that the coatings are non-absorbing (1.53+0i). While this might be appropriate for sulfate/nitrate rich shells it may not be nearly as robust if organic coatings contain brown carbon. Given that the authors are focusing on relative effects of multicore geometry vs. coating thickness, this may be an acceptable assumption, but they are encouraged to explicitly cite this simplifying assumption. Further, a sensitivity analysis as function of center vs. periphery vs. random position is encouraged to support the robustness of a 72% reduction claim.

Reply: Yes, if coatings on soot contain brown carbon, the optical characteristics of both coatings and soot-containing particles may change. As the reviewer commented, this study mainly focuses on relative effects of multicore geometry vs. coating thickness, so we simply assume the coating is non-absorbing. To clarify it, we have emphasized this simplified assumption for the optical simulation. We also added the sensitivity test to show the credibility of 72% $\Delta E_{abs}/\Delta(D_p/D_c)$ reduction (Figure S9).

P20 L530-532: “Moreover, the coatings of soot cores were assumed to be non-absorbing materials in the optical calculation.”

P23 L634-636: “Based on the optical simulation (assuming that coatings on soot are non-absorbing), transboundary soot-containing particles transported through the inland pathway exhibited a $\Delta E_{abs}/\Delta(D_p/D_c)$ of 0.6.”

P21-22 L575-583: “A sensitivity test was conducted for the $\Delta E_{abs}/\Delta(D_p/D_c)$ reduction caused by the transport pathway change through varying the embedded soot core position in host particles, as shown in Figure S9. It was found that the $\Delta E_{abs}/\Delta(D_p/D_c)$ reduction is 68% when soot cores are randomly distributed in host particles (Figure S9). This is close to the 72% reduction calculated when soot cores are distributed at the periphery of host particles (Figure S9). Because over 80% of the embedded soot cores were observed to be distributed at the periphery of transboundary particles, and the remainder was primarily randomly distributed, the 72% $\Delta E_{abs}/\Delta(D_p/D_c)$ reduction can be considered reliable.”

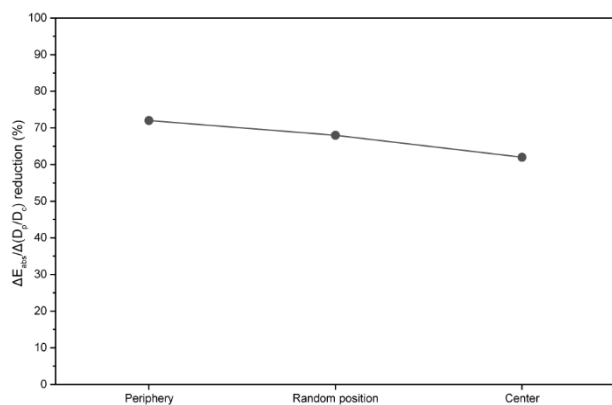


Figure S9. The $\Delta E_{abs}/\Delta(D_p/D_c)$ reduction of transboundary soot-containing particles with different core positions following the transport pathway change from the inland to the sea.

6. One of the take-home messages of this paper is that $\Delta E_{abs}/\Delta(D_p/D_c)$ is reduced by ~72% for sea-path soot because cloud processing generates multicore particles. This result is a model-derived result. Thus it might be useful to emphasize that $\Delta E_{abs}/\Delta(D_p/D_c)$ is a conceptual metric that depends on the chosen definition of D_p and D_c (e.g., equivalent sphere vs. outer droplet edge, etc.). This would underscore that while model–model comparison is likely

robust, model–measurement comparison would likely require careful matching of definitions.

Reply: We emphasized the $\Delta E_{abs}/\Delta(D_p/D_c)$ as a conceptual metric and its applicability.

P22 L590-593: “It should be noted that the $\Delta E_{abs}/\Delta(D_p/D_c)$ derived from optical simulation is a conceptual metric, which depends on the chosen definition of D_p and D_c (e.g., ESD). While model–model comparisons are likely robust, model–measurement comparisons would likely require careful matching of definitions.”

7. This reviewer was surprised by the rapid growth for the inland-route particles reported to reach 0.5–0.7 μm within a single transport episode. This is much larger than typically observed for non-cloud, early-age haze. To what degree is this a reflection of measurement bias - either through choice of methodology and/or selected size range vs actual growth that reflects intense secondary production? This is not to say that measurement bias invalidates the inland–sea comparison, but they suggest that the absolute size and coating metrics should be interpreted cautiously. The authors are encouraged to talk about this, especially in their comparisons with previous results that focused on sub-micron particles.

Reply: We apologize for any confusion caused to the reviewer regarding the interpretation that soot-containing particles transported through the inland pathway were mainly distributed within the broad size range of 500–700 nm in the YRD. Figure 5 actually shows the number percentage of soot-containing particles across different size bins. While the percentages were indeed high in both the 500–600 nm and 600–700 nm bins, the absolute number of soot-containing particles in the 500–600 nm range was approximately twice higher than that in the 600–700 nm range. This indicates that soot-containing particles were predominantly distributed around 500–600 nm, though this result remained a rough range. Further, we analyzed the number size distribution of soot-containing particles (Figure 6).

Based on the size distribution, the dominant size of soot-containing particles can be accurately determined. We added some discussion and revised the result as follows.

P15-16 L402-411: “The peak diameter at 505 nm for embedded soot-containing particles transported through the inland pathway is close to ~550 nm of aged soot-containing particles during regional haze reported by Wang et al. (2019). Although number fractions of these embedded soot-containing particles with 1 core were high in both the 500-600 nm and 600-700 nm bins (Figure 5b), the absolute number in the 500-600 nm range was approximately twice higher than that in the 600-700 nm range. As a result, the preponderant soot-containing particles in the YRD, i.e., embedded ones with 1 core (inland) and ≥ 3 cores (sea), dominated in the coarser size range of 500-600 nm and in the much coarser size range of > 1600 nm, respectively (Figure 5b, d).”

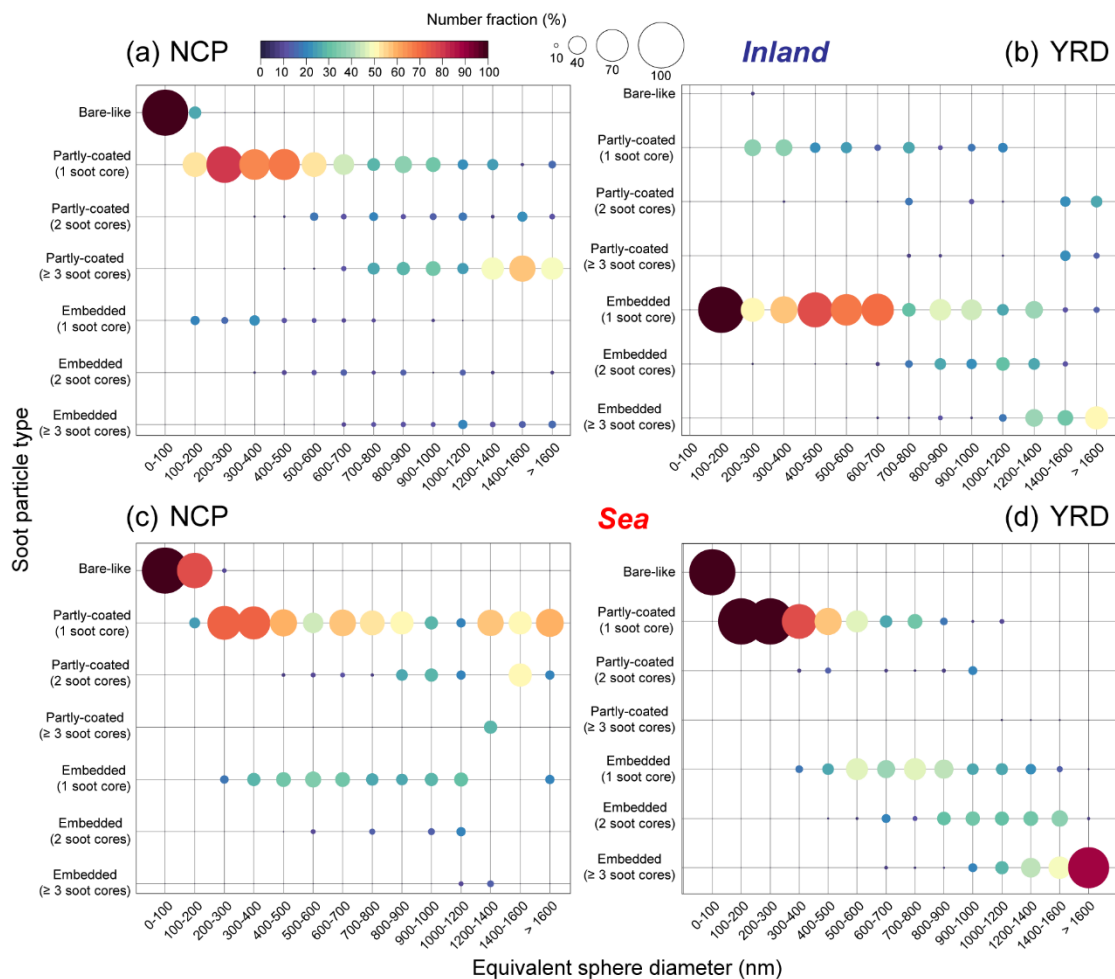


Figure 5. Number fractions of soot-containing particles with different mixing structures and numbers of soot cores in different size bins in two types of transboundary transport models from the NCP to the YRD. (a-b) Soot-containing particles transported through the inland pathway. (c-d) Soot-containing particles transported through the sea pathway.

8. Finally, this reviewer would also like urge caution on any quantitative comparisons to the submicron BC literature. It is well-documented that sub-micron soot acquires nm-scale coatings through condensation and heterogeneous chemistry with concomitant restructuring processes, whereas the super-micron particles, the size regime that this paper is focused on, form through cloud activation, aqueous growth, and droplet-scale coalescence, requiring a very different aging pathway. As a consequence, caution needs to be exercised when comparing metrics like D_p/D_c , D_f , and absorption enhancement from one regime to the other. Hence, the authors are encouraged to be explicit in treating their comparisons with sub-micron studies as qualitative.

Reply: We have carefully considered the comments and revised some quantitative comparisons into qualitative ones.

P17 L453-455: “Moreover, Xu et al. (2020) showed a relatively high D_p/D_c increase proportion of soot-containing particles during the transportation of dust storms from China across the East China Sea to Japan.”

P20 L548-551: “In addition, comparable radiative absorption changes for soot-containing particles with different numbers of soot cores were observed during the transformation of soot core positions (Zhang et al., 2022).”

9. Page 6, line 155; “...sampling duration of individual particles needs to be adjusted from 30 s to 15 min according to current PM2.5 concentrations.” Please cite the concentration range that dictated sampling durations that spanned the 30-sec to 15-min range.

Reply: We added the concentration range as follows.

P6 L155-157: “To avoid particles overlapping on the substrate, the sampling duration of individual particles needs to be adjusted from 30 s to 15 min according to current PM_{2.5} concentrations from 17 $\mu\text{g m}^{-3}$ to 320 $\mu\text{g m}^{-3}$.”

10. Page 15 (line 406)/Page 16 (line 407-408): “Soot particles have been demonstrated to promote the formation of secondary aerosols around them via heterogeneous or aqueous-phase reactions”. Soot is not a catalyst as implied in this sentence. Soot is chemically inert. Their primary role is as a non-reactive, insoluble substrate upon which material can be condensed onto. Please reword.

Reply: We reworded this sentence as follows.

P16-17 L435-437: “Soot particles have been demonstrated to provide a substrate for the formation of secondary aerosols via heterogeneous or aqueous-phase reactions (Farley et al., 2023; Han et al., 2013; Zhu et al., 2025).”

11. Figure 7: Please make the scale on the ordinate the same. It will help underscore just how difference the two ratios are. Also, as stated above, the authors might be serious consideration for using the mass ratio instead of Dp/Dc due to its independence of particle morphology.

Reply: The scales on the ordinates in Figure 7 were made same. We also added the V_{coating}/V_c ratio in Table S2.

References

Farley, R. N., Collier, S., Cappa, C. D., Williams, L. R., Onasch, T. B., Russell, L. M., Kim, H., and Zhang, Q.: Source apportionment of soot particles and aqueous-phase processing of black carbon coatings in an urban environment, *Atmos. Chem. Phys.*, 23, 15039-15056, <https://doi.org/10.5194/acp-23-15039-2023>, 2023.

Han, C., Liu, Y., and He, H.: Role of Organic Carbon in Heterogeneous Reaction of NO₂ with Soot, *Environ. Sci. Technol.*, 47, 3174-3181, <https://doi.org/10.1021/es304468n>, 2013.

Hou, X., Zhu, B., Kumar, K. R., de Leeuw, G., Lu, W., Huang, Q., and Zhu, X.: Establishment of Conceptual Schemas of Surface Synoptic Meteorological Situations Affecting Fine Particulate Pollution Across Eastern China in the Winter, *J. Geophys. Res.-Atmos.*, 125, e2020JD033153, <https://doi.org/10.1029/2020JD033153>, 2020.

Hu, X.-M., Hu, J., Gao, L., Cai, C., Jiang, Y., Xue, M., Zhao, T., and Crowell, S. M. R.: Multisensor and Multimodel Monitoring and Investigation of a Wintertime Air Pollution Event Ahead of a Cold Front Over Eastern China, *J. Geophys. Res.-Atmos.*, 126, e2020JD033538, <https://doi.org/10.1029/2020JD033538>, 2021.

Huang, X., Ding, A., Wang, Z., Ding, K., Gao, J., Chai, F., and Fu, C.: Amplified transboundary transport of haze by aerosol-boundary layer interaction in China, *Nat. Geosci.*, 13, 428–434, <https://doi.org/10.1038/s41561-020-0583-4>, 2020.

Li, M., Wang, T., Xie, M., Li, S., Zhuang, B., Huang, X., Chen, P., Zhao, M., and Liu, J.: Formation and Evolution Mechanisms for Two Extreme Haze Episodes in the Yangtze River Delta Region of China During Winter 2016, *J. Geophys. Res.-Atmos.*, 124, 3607-3623, <https://doi.org/10.1029/2019JD030535>, 2019.

Liu, L., Zhang, J., Xu, L., Yuan, Q., Huang, D., Chen, J., Shi, Z., Sun, Y., Fu, P., Wang, Z., Zhang, D., and Li, W.: Cloud scavenging of anthropogenic refractory particles at a mountain site in North China, *Atmos. Chem. Phys.*, 18, 14681-14693, <https://doi.org/10.5194/acp-18-14681-2018>, 2018.

Wang, J., Liu, D., Ge, X., Wu, Y., Shen, F., Chen, M., Zhao, J., Xie, C., Wang, Q., Xu, W., Zhang, J., Hu, J., Allan, J., Joshi, R., Fu, P., Coe, H., and Sun, Y.: Characterization of black carbon-containing fine particles in Beijing during wintertime, *Atmos. Chem. Phys.*, 19, 447-458, <https://doi.org/10.5194/acp-19-447-2019>, 2019.

Wu, J., Bei, N., Li, X., Wang, R., Liu, S., Jiang, Q., Tie, X., and Li, G.: Impacts of Transboundary Transport on Coastal Air Quality of South China, *J. Geophys. Res.-Atmos.*, 127, e2021JD036213, <https://doi.org/10.1029/2021JD036213>, 2022.

Xie, X., Hu, J., Qin, M., Guo, S., Hu, M., Ji, D., Wang, H., Lou, S., Huang, C., Liu, C., Zhang, H., Ying, Q., Liao, H., and Zhang, Y.: Evolution of atmospheric age of particles and its implications for the formation of a severe haze event in eastern China, *Atmos. Chem. Phys.*, 23, 10563-10578, <https://doi.org/10.5194/acp-23-10563-2023>, 2023.

Xu, L., Fukushima, S., Sobanska, S., Murata, K., Naganuma, A., Liu, L., Wang, Y., Niu, H., Shi, Z., Kojima, T., Zhang, D., and Li, W.: Tracing the evolution of morphology and mixing state of soot particles along with the movement of an Asian dust storm, *Atmos. Chem. Phys.*, 20, 14321-14332, <https://doi.org/10.5194/acp-20-14321-2020>, 2020.

Zhang, J., Yuan, Q., Liu, L., Wang, Y., Zhang, Y., Xu, L., Pang, Y., Zhu, Y., Niu, H., Shao, L., Yang, S., Liu, H., Pan, X., Shi, Z., Hu, M., Fu, P., and Li, W.: Trans-Regional Transport of Haze Particles From the North China Plain to Yangtze River Delta During Winter, *J. Geophys. Res.-Atmos.*, 126, e2020JD033778, <https://doi.org/10.1029/2020JD033778>, 2021.

Zhang, J., Wang, Y., Teng, X., Liu, L., Xu, Y., Ren, L., Shi, Z., Zhang, Y., Jiang, J., Liu, D., Hu, M., Shao, L., Chen, J., Martin, S. T., Zhang, X., and Li, W.: Liquid-liquid phase separation reduces radiative absorption by aged black carbon aerosols, *Commun. Earth Environ.*, 3, 128, <https://doi.org/10.1038/s43247-022-00462-1>, 2022.

Zhang, J., Li, W., Wang, Y., Teng, X., Zhang, Y., Xu, L., Yuan, Q., Wu, G., Niu, H., and Shao, L.: Structural Collapse and Coating Composition Changes of Soot Particles During Long-Range Transport, *J. Geophys. Res.-Atmos.*, 128, e2023JD038871, <https://doi.org/10.1029/2023JD038871>, 2023.

Zhu, J., Wu, S., Yue, H., Gao, E., Wang, W., Li, J., Wu, Z., and Yao, S.: Enhanced oxidative potential and SO₂ heterogeneous oxidation on candle soot after photochemical aging: Influencing mechanisms of different irradiation wavelengths, *Environ. Pollut.*, 367, 125583, <https://doi.org/10.1016/j.envpol.2024.125583>, 2025.